AIAA JOURNAL
Vol. 36, No. 1, January 1998

Flutter Prediction Using an Eigenvector Orientation Approach

Daré Afolabi* and Ramana M. V. Pidaparti†
Purdue University at Indianapolis, Indianapolis, Indiana 46202-5132
and
Henry T. Y. Yang‡
University of California, Santa Barbara, Santa Barbara, California 93106-2030

A method for predicting the onset of coupled-mode flutter is presented. A distinguishing characteristic of this method is that it emphasizes eigenvectors rather than eigenvalues. In the popular methods based on eigenvalues, flutter is predicted as instability begins to occur, as evidenced by the movement of one or more eigenvalues from the left-hand to the right-hand side of the *s*-plane, or the coalescence of eigenvalues. Alternatively, the method of eigenvector orientation being presented has the potential to predict the occurence of instability. Although the eigenvectors of vibrating systems generally satisfy the orthogonality condition, there are certain cases in aeroelasticity in which they are not orthogonal. In a typical case of coupled-mode flutter, the eigenvectors initially may be oriented orthogonally but gradually lose orthogonality as airspeed is varied. The consequence of such a progressive loss of eigenvector orthogonality on structural dynamics is a phenomenon that seems to warrant further investigation. This investigation has applications in areas such as helicopter dynamics, aeroelastic analysis of plate and shell structures, analysis of slightly mistuned bladed disk assemblies, and rotordynamics.

I. Introduction

In aeroelasticity, there are certain situations in which it is desirable to study the dynamics of a system in terms of one dominant parameter, which can be called the system parameter. An example of such a parameter is the airspeed U, in the classical coupled bending-torsion of a wing section in an airstream. At the reference or datum state of the system parameter, e.g., when the airspeed $U = 0$, eigenvectors are often found to be orthogonal. However, as the system parameter changes under operating conditions, the eigenvectors gradually cease to be orthogonal. Initially, this loss of orthogonality appears to be insignificant, and can be ignored in flutter prediction. However, there are times when the loss of orthogonality is of such a magnitude that considerable qualitative and quantitative errors may be incurred by assuming that orthogonality continues to hold. The consequence of a gradual loss of orthogonality of eigenvectors on the structural dynamics of an aeroelastic system is a phenomenon that warrants more in-depth studies.

Discussion is given first to some of the consequences of a gradual loss of orthogonality of eigenvectors on structural dynamics. Although the primary aim of this study is the effect of eigenvector orientation on the onset of flutter, there are other dynamic characteristics, such as forced response, that may be affected by the nonorthogonality of eigenvectors. This is evident from modal analysis because it is well known that the forced response of a linear vibrating system can be computed as a weighted sum of eigenvectors, via the process of modal summation. Orthogonality of eigenvectors normally is assumed in such a process. However, although the eigenvectors of most vibrating systems are orthogonal, it is illustrated in this study that the eigenvectors are not always orthogonal in certain aeroelastic systems in which the eigenmatrices depend on a system parameter, such as airspeed or Mach number.

The onset of flutter is normally determined by tracking the eigenvalues, as the least stable mode moves from the left-hand to the right-hand side of the *s*-plane, or as a coalescence occurs between two or more eigenvalues. A distinguishing characteristic of this investigation is that the eigenvectors are used to predict the onset of flutter, as an alternative approach. The approach is useful in making a prediction in situations in which two or more modes interact to induce flutter, a condition normally known as coupled-mode flutter.

Received Dec. 14, 1996; revision received Sept. 12, 1997; accepted for publication Sept. 15, 1997.

*Associate Professor, Department of Mechanical Engineering, 723 West Michigan Street.
†Associate Professor, Department of Mechanical Engineering, 723 West Michigan Street. Associate Fellow AIAA.
‡Professor of Mechanical Engineering and Chancellor. Fellow AIAA.

II. Preliminaries

A. Conservative and Nonconservative Coupling

In investigating the influence of nonorthogonality of eigenvectors on structural dynamics, it is useful to utilize the classification of vibrating systems into two categories, depending on the nature of coupling within the system, as introduced by Crandall and Mroszczyk.[1] The two types of coupling are called conservative and nonconservative. Conservative coupling implies that the eigenvalue matrix can always be transformed into a symmetric form. Conversely, nonconservative coupling implies that the eigenmatrix cannot be made symmetric by matrix transformation procedures such as the methods of Jacobi or Givens, well known in numerical analysis. Often, but not always, this means that the eigenmatrix has an intrinsic skew symmetric or symplectic structure, in contrast to a symmetric or Euclidean structure. The conservatism referred to here concerns coupling, and not necessarily the conservation of energy of the vibrating system. Because matrix techniques frequently are used in vibration analysis, the nature of coupling in a model is determined by inspecting the off-diagonal or coupling elements in the eigenvalue matrix. If the coupling terms imply a symmetric structure, then it is conservative coupling. If the coupling terms imply a skew symmetric structure, then it is nonconservative coupling. In some other cases of arbitrary matrix structure, the determination of the type of coupling may not be apparent by mere inspection. These concepts of conservative coupling and nonconservative coupling have been used to study the flutter of rotating blades.[2]

The equation of motion for the free vibration of an undamped system normally is formulated in a space with physical coordinates $\{x\}$. Alternatively, one also may formulate the problem in modal coordinates $\{\phi\}$:

$$[M_x]\{\ddot{x}\} + [K_x]\{x\} = 0 \tag{1a}$$

$$[M_\phi]\{\ddot{\phi}\} + [K_\phi]\{\phi\} = 0 \tag{1b}$$

Although solution in modal space may not be as common as solution in physical space, there are some attractive reasons for using

the modal-space formulation. In physical coordinates x, the degree of freedom (DOF) may be very large, say several hundreds or perhaps thousands, whereas only a few DOF are needed if the problem is analyzed in modal coordinates. For instance, if the coupled bending-torsion vibrations of an aeroelastic structure are considered, two DOF may be sufficient in the modal-space formulation for the purpose of analytical demonstration. Significantly reducing the DOF associated with a given problem may simplify the derivation of closed-form solutions for parametric studies in which one investigates the dependence of solution on various parameters of interest.

Equation (1b) may be reduced to an eigenvalue problem,

$$[A]\{\phi\} = \lambda\{\phi\} \tag{2}$$

The eigenmatrix $[A]$ of a system without damping has real elements. For coupled bending-torsion vibrations, $[A]$ is a 2×2 matrix in modal space spanned by the bending $\{\phi_B\}$ and torsion $\{\phi_T\}$ coordinates. Such eigenmatrices frequently are encountered in various stability problems of vibration analysis, and a classification has been made by Crandall and Mroszczyk[1] in the course of their investigations on rotating machinery. According to the classification, one can identify two categories: an eigenmatrix for systems with conservative coupling with a canonical representation

$$[A_c] = \begin{bmatrix} 1-\alpha & -\gamma \\ -\gamma & 1+\alpha \end{bmatrix} \tag{3a}$$

and an eigenmatrix for systems with nonconservative coupling,

$$[A_n] = \begin{bmatrix} 1-\alpha & -\gamma \\ \gamma & 1+\alpha \end{bmatrix} \tag{3b}$$

In the foregoing, γ is both a qualitative and a quantitative measure of the coupling in the system. The magnitude of γ is a measure of the strength of coupling, whereas the relative signs of the off-diagonal terms have qualitative significance. An eigenmatrix with real elements $a_{ij} = a_{ji}$ implies conservative coupling, whereas $a_{ij} = -a_{ji}$ implies nonconservative coupling.

It is sometimes more convenient to work with noncanonical forms of eigenmatrices. For instance, if the mass matrix is a unit matrix, then one can write noncanonical representations of Eqs. (3a) and (3b), respectively, in the forms

$$[A_c] = \begin{bmatrix} k_0-\alpha & -\gamma \\ -\gamma & k_0+\alpha \end{bmatrix} \tag{4a}$$

and

$$[A_n] = \begin{bmatrix} k_0-\alpha & -\gamma \\ \gamma & k_0+\alpha \end{bmatrix} \tag{4b}$$

where k_0 denotes the nominal stiffness, α denotes mistuning or imperfection parameters, and γ is a coupling factor, as before.

By distinguishing between conservative γ_c and nonconservative γ_n coupling parameters, and translating the origin in the parameter space relative to the axis represented by the parameter α, one can recast the above as follows. For the conservative coupling case,

$$[A_c] = \begin{bmatrix} k_0-\alpha_0+\alpha & -\gamma_c \\ -\gamma_c & k_0+\alpha_0-\alpha \end{bmatrix} \tag{5a}$$

and, for the nonconservative coupling case,

$$[A_n] = \begin{bmatrix} k_0-\alpha_0+\alpha & -\gamma_n \\ \gamma_n & k_0+\alpha_0-\alpha \end{bmatrix} \tag{5b}$$

An illustration of how nonconservative coupling arises naturally in aeroelasticity is furnished by the problem of panel flutter at high supersonic Mach numbers; see, for instance, the book by Dowell.[3] By using Galerkin's procedure, it can be shown that the equation of motion of a fluttering plate can be cast in the form

$$m_n\left(\omega_n^2 q_n + \frac{\mathrm{d}^2 q_n}{\mathrm{d}t^2}\right) + \rho_\infty U_\infty^2 Q_n = 0 \tag{6}$$

where $n = 1, \ldots, \infty$ denotes a mode of vibration, and Q_n arises from aerodynamic coupling of modes. By taking Fourier transforms, one converts Eq. (6) to the frequency domain to get

$$\{\bar{Q}^E\} = \frac{1}{\rho_\infty U_\infty^2}[K]\{q\} \tag{7}$$

where $[K]$ can be regarded as a dynamic stiffness matrix. For a two-mode approximation as shown in Ref. 3 [p. 20, Eq. (27)], this yields the stiffness matrices

$$[K] = \begin{bmatrix} m_1(\omega_1^2 - \omega^2) & \rho_\infty U_\infty^2 \bar{Q}_{21}^M \\ -\rho_\infty U_\infty^2 \bar{Q}_{21}^M & m_2(\omega_2^2 - \omega^2) \end{bmatrix} \tag{8}$$

The skew symmetric coupling characteristic of nonconservative systems is evident in the stiffness matrix displayed in Eq. (8).

B. Orbits of Matrices Dependent on Parameters

Many problems in flutter analysis, especially those involving a coupling of two or more modes of vibration, can be formulated in terms of matrices dependent on parameters. A definitive study of matrices dependent on parameters has been made by Arnol'd.[4] As the system parameters are varied, a family of matrices arises. These matrices can be classified by means of the equivalence relation inherent in the procedure of similarity transformation of matrices. Each equivalence class of similar matrices $\{A : A = U^{-1}BU\}$ defines an orbit under the action of the general linear group $GL(n, \mathbb{R})$. An important result that can be deduced from the work of Arnol'd[4] is that an encounter with degenerate eigenvalues in the study of a family of matrices dependent on parameters is significant because it indicates a loss of transversality at the intersection of one or more orbits in the parameter space.

A loss of transversality is important because, for applications, it indicates a qualitative change in dynamics. Thus, loss of elastic stability, the incidence of bifurcation of dynamic states, or the coalescence of modes occur when a loss of transversality is encountered in a dynamic system dependent on parameters.

The relevance of the foregoing to the problem of coupled-mode flutter is eigenvalue degeneracy. When two or more modes coalesce at the onset of flutter, an eigenvalue degeneracy is induced, and a mathematical loss of transversality occurs. The phenomenon of coalescence is, in essence, a duality of the phenomenon of bifurcation. In the former case, two previously distinct modes fuse to become one; in the latter case, a single mode separates or splits into two distinct modes. The unifying factor of these two phenomena is transversality. A detailed study of the role of transversality in flutter analysis is given in Ref. 5.

III. Eigenvectors of Matrices with Parametric Dependence

In many flutter problems, the characteristic instability is due to nonconservative coupling, giving rise to a coalescence of two modes. The modes are ordinarily distinct when there is stability, but lose their identity at the onset of flutter. In this section, it is shown that the angle between the two eigenvectors—or, equivalently, the orientation of eigenvectors—can be used to predict the onset of flutter. This seems to be an alternative approach to the popular practice in which the onset of flutter is based on the coalescence of eigenvalues.[6–9]

A. Angle Between Two Complex Eigenvectors

It appears straightforward to compute the angle between two real vectors of dimension n from their scalar product. Thus, if $\{v_1, v_2 \in \mathbb{R}^n\}$ are two such vectors, the angle in question is the arc-cosine,

$$\theta = \cos^{-1}\left(\frac{v_1 \cdot v_2}{\|v_1\|\,\|v_2\|}\right) = c_{12} \tag{9}$$

It does not appear that a universal method exists for computing the angle between two complex vectors, or for interpreting what the geometric meaning of such an angle might be. Extending the definition for the real case to cover $\{v_1, v_2 \in \mathbb{C}^n\}$ is neither unique nor straightforward. Several approaches suggest themselves. The

simplest way is to replace the scalar product in Eq. (9) with the Hermitian scalar product, i.e., replace one of the vectors by its complex conjugate before computing their scalar product; thus,

$$c_{ij} = \frac{\bar{v}_i \cdot v_j}{||\bar{v}_i||\,||v_j||} \tag{10}$$

where an overbar denotes complex conjugation. The problem with Eq. (10) is that the computed scalar c_{ij} is not necessarily real, and finding the angle whose cosine is a complex scalar is impossible.

A practical solution seems to be a mapping of $\mathbb{C}^n$–$\mathbb{R}^{2n}$, sometimes known as realification, the inverse mapping being a complexification. What this entails is that one strings out the components of v_i, placing the imaginary components after the real. In the process, one obtains a real vector of dimension $2n$ from a complex vector of dimension n. This device was employed recently[10] to compute the angle between two eigenvectors, which may be real initially, but may later become complex as the parameters on which the eigenvectors depend are varied.

B. Conservative Coupling

A system with conservative coupling is characterized by a symmetric eigenmatrix, if all of the off-diagonal terms are real. For the real, symmetric eigenmatrix in Eq. (5a), its eigenvalues can be written as

$$\lambda_1^{(c)} = k_0 - \sqrt{(\alpha-\alpha_0)^2 + \gamma_c^2}$$
$$\lambda_2^{(c)} = k_0 + \sqrt{(\alpha-\alpha_0)^2 + \gamma_c^2} \tag{11}$$

where the superscript c indicates conservative coupling. For small values of γ_c, the approximate expressions for the eigenvalues are

$$\lambda_1^{(c)} = k_0 - (\alpha-\alpha_0) - \frac{\gamma_c^2}{2(\alpha-\alpha_0)}$$
$$\lambda_2^{(c)} = k_0 + (\alpha-\alpha_0) + \frac{\gamma_c^2}{2(\alpha-\alpha_0)} \tag{12}$$

If the corresponding eigenvectors are denoted by u_1^c and u_2^c, respectively, then

$$u_1^{(c)} = \left\{\gamma_c \quad (\alpha-\alpha_0) + \sqrt{(\alpha-\alpha_0)^2+\gamma_c^2}\right\}^T \tag{13a}$$

$$u_2^{(c)} = \left\{\gamma_c \quad (\alpha-\alpha_0) - \sqrt{(\alpha-\alpha_0)^2+\gamma_c^2}\right\}^T \tag{13b}$$

Note that the eigenvectors above are independent of the nominal stiffness, k_0. As γ_n approaches zero, the approximate representations of the eigenvectors are

$$u_1^{(c)} = \begin{Bmatrix}\gamma_c \\ 2(\alpha-\alpha_0)\end{Bmatrix} \tag{14a}$$

$$u_2^{(c)} = \begin{Bmatrix}2(\alpha-\alpha_0) \\ -\gamma_c\end{Bmatrix} \tag{14b}$$

If all of the parameters α, α_0, γ_c, and k_0 are real quantities, then one can obtain an expression for the angle between the eigenvectors in Eq. (10), for all values of the parameters, as

$$\cos\theta_c = 0 \tag{15}$$

Hence, the eigenvectors are always orthogonal. This well-known result for a system with conservative coupling can be used as a reference or benchmark against which the result for a system with nonconservative coupling could be compared.

The variation of eigenvalues with the system parameter γ is illustrated in Fig. 1a, whereas the relationship of the angle between the two eigenvectors and the parameter γ is shown in Fig. 1b.

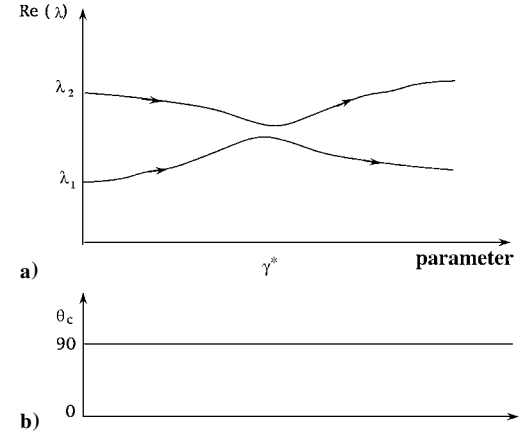

Fig. 1 Variation of a) eigenvalues λ and b) angle between eigenvectors θ_c as functions of the coupling parameter γ in a system with conservative coupling.

C. Nonconservative Coupling

The eigenvalues of the eigenmatrix in Eq. (5b) are easily obtained, and can be cast in the form

$$\lambda_1^{(n)} = k_0 - \sqrt{(\alpha-\alpha_0)^2 - \gamma_n^2}$$
$$\lambda_2^{(n)} = k_0 + \sqrt{(\alpha-\alpha_0)^2 - \gamma_n^2} \tag{16}$$

where the superscript n indicates nonconservative coupling. For small values of γ_n, the approximate expressions for the eigenvalues are

$$\lambda_1^{(n)} = k_0 - (\alpha-\alpha_0) + \frac{\gamma_n^2}{2(\alpha-\alpha_0)}$$
$$\lambda_2^{(n)} = k_0 + (\alpha-\alpha_0) - \frac{\gamma_n^2}{2(\alpha-\alpha_0)} \tag{17}$$

If the corresponding eigenvectors are denoted by u_1^n and u_2^n, respectively, then

$$u_1^n = \left\{\gamma_n \quad (\alpha-\alpha_0) + \sqrt{(\alpha-\alpha_0)^2-\gamma_n^2}\right\}^T \tag{18a}$$

$$u_2^n = \left\{\gamma_n \quad (\alpha-\alpha_0) - \sqrt{(\alpha-\alpha_0)^2-\gamma_n^2}\right\}^T \tag{18b}$$

Note that the eigenvectors in Eqs. (18a) and (18b) are independent of the nominal stiffness, k_0. As γ_n approaches zero, the approximate representations of the eigenvectors are

$$u_1^n = \begin{Bmatrix}\gamma_n \\ 2(\alpha-\alpha_0)\end{Bmatrix}, \qquad u_2^n = \begin{Bmatrix}2(\alpha-\alpha_0) \\ \gamma_n\end{Bmatrix} \tag{19}$$

If all of the parameters α, α_0, γ_n, and k_0 are real quantities, then one can obtain an expression for the angle between the eigenvectors in Eq. (19) as

$$\cos\theta_n = \frac{\gamma_n}{|\alpha-\alpha_0|} \tag{20}$$

In the case in which the eigenvectors acquire imaginary components, one can use the procedure devised in Eq. (10) to compute the required angle.

As in the preceding case of conservative coupling, one can sketch the variation of the real and imaginary parts of the eigenvalues and angle between eigenvectors as a function of the parameter γ, as illustrated in Fig. 2. It is evident that, within the flutter zone, the notion of an angle between the eigenvectors breaks down.

IV. Applications

These concepts and derivations are illustrated and evaluated by performing the analysis of a set of examples of panel flutter. An isotropic plate, an orthotropic laminated composite square plate, and an isotropic and a composite cylindrical shell with various boundary conditions are considered. The square plates have simply supported

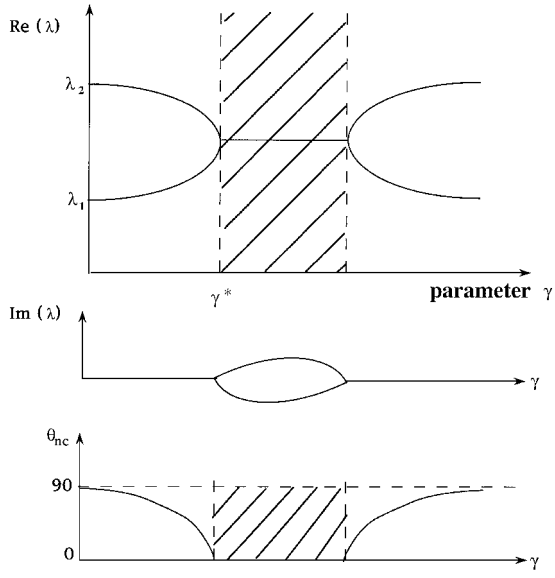

Fig. 2 Variation of eigenvalues λ and angle between eigenvectors θ_c as functions of the coupling parameter γ in a system with nonconservative coupling.

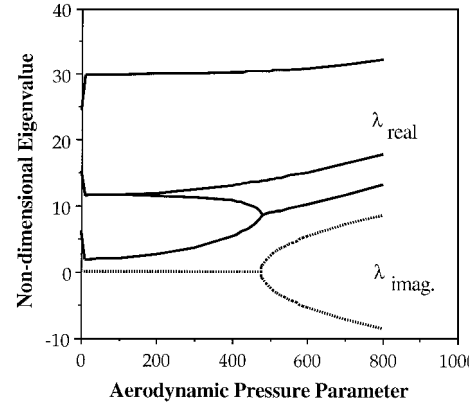

Fig. 3 Eigenvalues of the isotropic plate as functions of the coupling parameter.

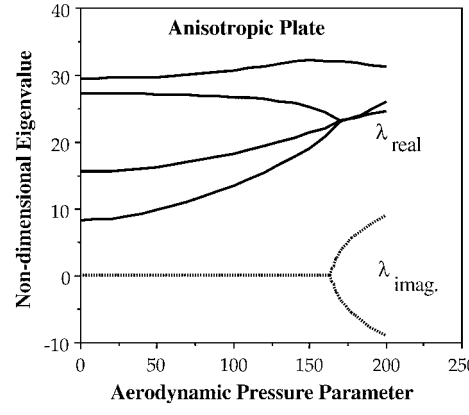

Fig. 4 Eigenvalues of the composite plate as functions of the coupling parameter.

boundary conditions, whereas the cylindrical shell is clamped on all edges. The geometry of both square plates was the same, assumed as length or width (a) = 10 in. and thickness (h) = 0.1 in. The material properties for the isotropic plate were assumed to be modulus of elasticity $E = 10$ Mpsi, Poisson's ratio $\nu = 0.3$, and mass density $\rho = 0.025$ lb-s^2/in.[4] For the laminated composite plate with unidirectional 0-deg/90-deg fiber orientation, the material properties were assumed to be $E_1/E_2 = 5$, $G_{12}/E_{12} = 0.4$, $\nu_{12} = 0.25$, and $\rho = 0.0025$ lb-s^2/in.[4] The eigenvalue results are nondimensionalized using $[\lambda a^2(\rho h/E^* h^3)^{1/2}]$ and presented in subsequent figures; $E^* = E$ for the isotropic case, and $E^* = E_2$ for the composite examples.

Both plates and cylindrical curved panels, made from isotropic and composite materials, were modeled and analyzed using a high-precision 48-DOF curved-shell finite element.[9,11] This element also was used for the analysis of flat panels by simply setting the radii of curvature to be zero and suppressing those unnecessary in-plane-related DOF. The present finite element is quadrilateral in shape, and has four corner nodal points with 12 DOF at each node: $u, u_x, u_y, u_{xy}, v, v_x, v_y, v_{xy}, w, w_x, w_y, w_{xy}$, where u, v, and w are displacements in the curvilinear directions x, y, and z, respectively, and the subscripts x and y indicate derivatives. The element stiffness matrix was formulated on the basis of classical lamination theory and the aerodynamic matrix was based on a linearized piston theory for supersonic flutter analysis. Details of the finite element formulation can be found in Refs. 11 and 12. The shell panels were analyzed for free vibration by use of a series of successively refined meshes, i.e., 4 × 4, 6 × 6, and 8 × 8. It was found that the first four frequencies reached a set of converged values at the level of 6 × 6 mesh (588 DOF without constraints) within a variation of about 1%. Needless to say, 6 × 6 mesh is sufficiently refined and converged for the free vibration analyses of the present flat-panel example. Thus, a 6 × 6 mesh was used throughout all of the panel examples, both flat and curved, in the present analyses.

The free-vibration modes in these examples are similar to those found by Pidaparti and Yang.[11] In this study, the size of the dynamic matrices from the previous analysis[11] was reduced from 588 × 588 to 10 × 10 using modal coordinates. The flutter analysis is carried out in modal coordinates to find the critical aerodynamic parameter.

Figures 3 and 4 show the variation of eigenvalues for the four fundamental modes as a function of the aerodynamic pressure parameter β for the isotropic plate and the composite plate, respectively. The aerodynamic pressure parameter is defined in Ref. 11 as

$$\beta = \frac{2q}{\sqrt{M_\infty^2 - 1}} \tag{21}$$

where M_∞ denotes Mach number and q is the freestream dynamic pressure. The foregoing analysis is applicable for the range of airspeed for which linear aerodynamic modeling is admissible. An analysis of the orientation of eigenvectors under the more general condition of nonlinear aerodynamics is much more complex than the preceding treatment and requires further investigation. For a general treatment of nonlinear flows, see, for example, Ref. 13.

It can be seen that eigenvalues 1 and 2 coalesce for the isotropic plate, whereas eigenvalues 2 and 3 coalesce for the composite plate. It can be seen from Figs. 3 and 4 that flutter takes place around a critical value of aerodynamic parameter of $\beta^* = 480$ and 166 for the isotropic and composite plates, respectively. It is of interest to examine the eigenvectors corresponding to these four fundamental eigenvalues for both of the cases in Figs. 3 and 4. Figures 5 and 6 show the real and imaginary components of the eigenvectors plotted as arrow-headed vectors for the four modes at three different values of aerodynamic parameter. The horizontal axis in each cell of the figures indicates the real part of the complex valued vector; the vertical axis indicates the imaginary part of the complex eigenvector. It can be seen from Fig. 5 that eigenvectors for the four modes are real at an aerodynamic parameter of 200. When the aerodynamic parameter is 480, modes 1 and 2 exhibit complex eigenvectors. This phenomenon means that modes 1 and 2 are participating in the dynamics in such a way as to give rise to a flutter condition. At an aerodynamic parameter of 700, modes 1 and 2 exhibit a greater participation in the flutter after its initiation. Results similar to those for the isotropic plate were observed for the composite plate, as shown in Fig. 6. Modes 2 and 3 first coalesced at $\beta = 166$ when the eigenvectors become complex. At an aerodynamic parameter of 200, mode 3 exhibits a phase change after the flutter condition. It can be seen from Figs. 5 and 6 that, if flutter occurs at a critical value of the parameter β^*, then the eigenvectors are real for values of $\beta < \beta^*$, but become complex within the flutter zone.

Figures 7 and 8 show the variation of the angle θ between the two eigenvectors (modes 1 and 2) for the isotropic plate and the two eigenvectors (modes 2 and 3) for the composite plate, respectively, during and after the coupling of modes. It can be seen from Fig. 7 that the angle θ drops gradually to zero as the isotropic plate approaches

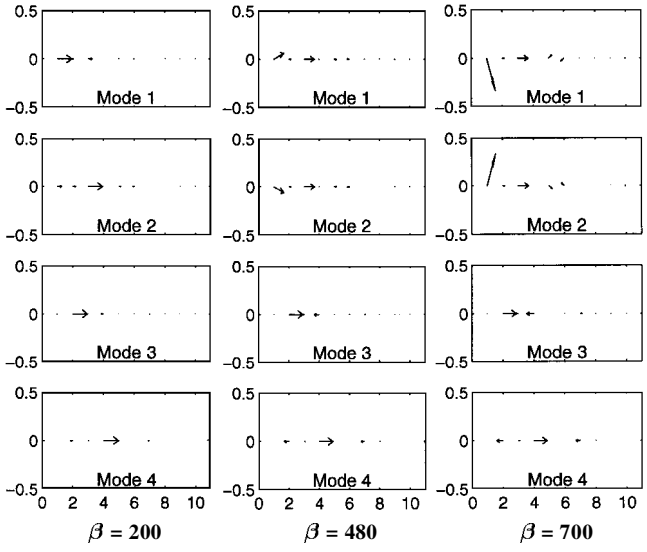

Fig. 5 Eigenvectors for first four modes at three different aerodynamic parameters β for the isotropic plate.

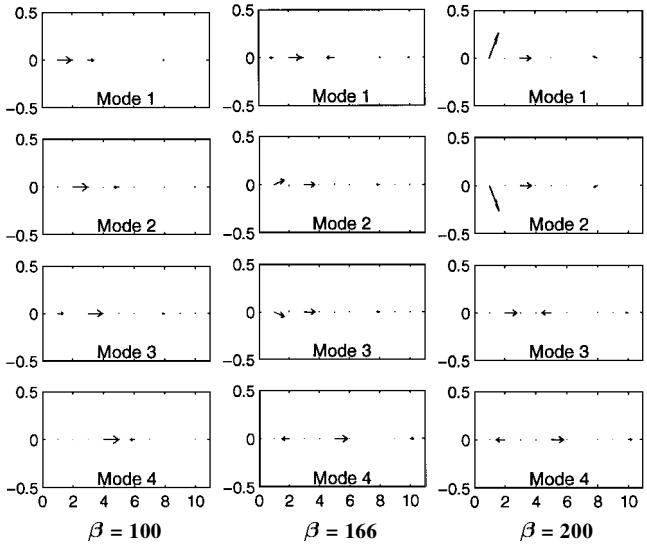

Fig. 6 Eigenvectors for first four modes at three different aerodynamic parameters β for the composite plate.

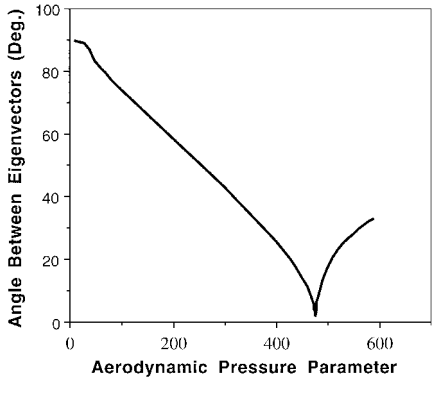

Fig. 7 Angle between eigenvectors of modes 1 and 2 for isotropic plate as functions of aerodynamic parameter.

the flutter condition. However, for the composite plate, the angle θ drops steeply as the plate approaches the flutter condition (Fig. 8). The fact that the angle between any pair of eigenvectors is not uniformly 90 deg in either case implies that the eigenvectors have started to lose their orthogonality. In both Figs. 7 and 8, the angle between those interacting eigenvectors giving rise to coupled-mode flutter clearly is not orthogonal as the aerodynamic parameter changes. The two eigenvectors participating in the coupled-mode flutter become less orthogonal, at a progressively rapid rate, before flutter

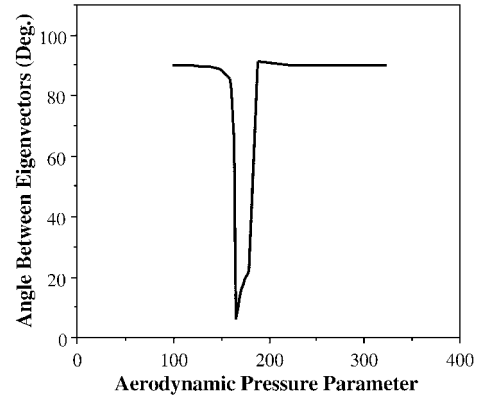

Fig. 8 Angle between eigenvectors of modes 2 and 3 for composite plate as functions of aerodynamic parameter.

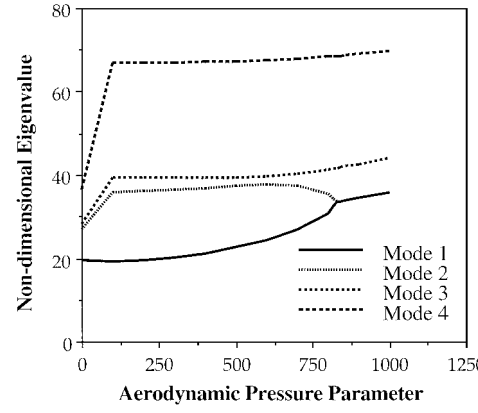

Fig. 9a Eigenvalues of the cylindrically curved isotropic panel as functions of aerodynamic parameter.

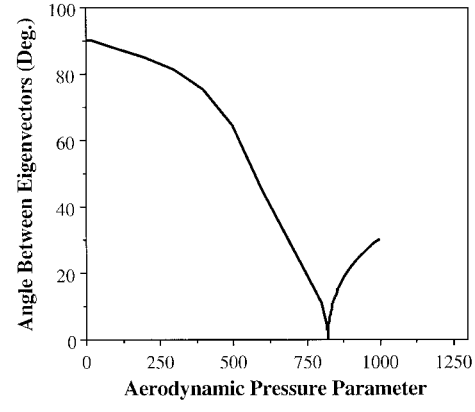

Fig. 9b Angle between eigenvectors of modes 1 and 2 for cylindrically curved isotropic panel as functions of aerodynamic parameter.

really occurs. On the contrary, in a comparable situation, systems with purely conservative coupling generally exhibit orthogonality of eigenvectors throughout the range of values when the systems' parameters are varied.

To further illustrate the eigenvector orientation approach, examples of isotropic and composite shell panels were considered. The assumed geometry for both the isotropic and composite panel was defined as the ratio between radius to longitudinal length = 20, longitudinal length $l = 10$ in., thickness $h = 0.01$ in. The composite panel was assumed to have 0-deg/90-deg lamination, with material properties similar to those of the composite plate. The curved panels were analyzed by successively refining the meshes (8×8, 6×6, and 4×4) and observing their convergence trends. It was found that the four lowest natural frequencies converged at a mesh level of 6×6 within a variation of about 1%.[11] Ten free-vibration modes were used to find the flutter boundary.

Figure 9a shows the variation of eigenvalues for the first four modes for the isotropic cylindrical panel as a function of the

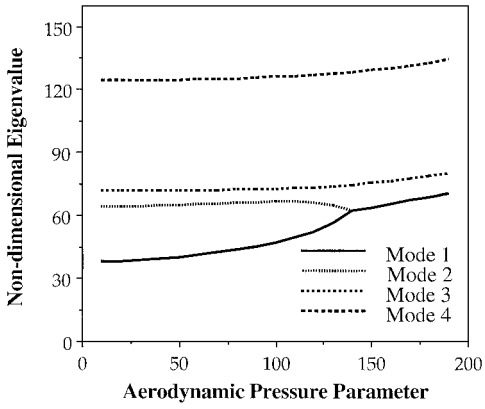

Fig. 10a Eigenvalues of the curved composite shell panel as functions of the aerodynamic parameter.

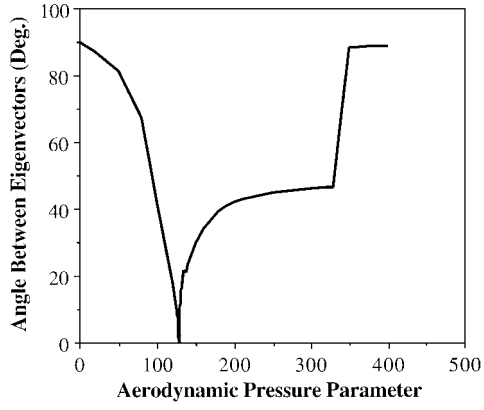

Fig. 10b Angle between the eigenvectors of modes 1 and 2 for the composite panel as functions of the aerodynamic parameter.

aerodynamic parameter β. Eigenvalues for modes 1 and 2 coalesce and give rise to the flutter condition around a critical value of aerodynamic parameter $\beta^* = 820$. The variation of the angle θ between the two eigenvectors (modes 1 and 2) is shown in Fig. 9b as a function of the aerodynamic parameter β. The rate of change of the angle between the two eigenvectors drops gradually to zero in the neighborhood of $\beta^* = 820$. A similar rate of gradual change can be observed for the isotropic plate (Fig. 7).

For the composite cylindrical panel, the variation of eigenvalues for the first four modes as a function of the aerodynamic parameter β is shown in Fig. 10a. Once again, the coalescence takes place between modes 1 and 2. Figure 10b shows the variation of the angle θ between modes 1 and 2 for this composite panel during and after the coalescence. It can be seen from Fig. 10b that the angle θ drops sharply to zero as the panel approaches the flutter condition. The qualitative rate of change of the angle between eigenvectors is sharper than that observed for the isotropic panel in Fig. 9b.

At a flutter boundary in a coupled-mode flutter situation, the angle between the eigenvectors of the two modes participating in the flutter becomes zero. Thus, at the critical value of the aerodynamic parameter, the two modes share identical geometric orientation, as the eigenspace collapses dramatically and discretely from a vector space of size $2n$ to a space of size n. Note that, before flutter actually occurs, the eigenvectors begin to signal the impending occurence of flutter by gradually losing their orthogonality. Therefore, the extent to which the angle between the pair of interacting eigenvectors deviates from 90 deg indicates the extent to which the system is close to a flutter boundary. Consequently, the magnitude of the angle between the eigenvectors, or its deviation from 90 deg, can be used as an indicator of the onset of flutter. The present approach to panel flutter problems is based on an extension of the method of nonconservative coupling developed by Crandall and Mroszczyk[1] for various instability problems in rotordynamics. From Ref. 1, the present method has arisen using eigenvector orientation as a method of flutter prediction. Its applicability for panel flutter analysis, using examples of isotropic and composite panels, both flat and curved, has been demonstrated.

V. Conclusions

A method for predicting the onset of coupled-mode flutter using an eigenvector orientation approach has been given. Examples of isotropic and composite flat plates and cylindrical curved panels are given. The examples demonstrate the usefulness of the present approach for predicting flutter. The rate of change of the angle between eigenvectors is another indication of how the flutter condition is approached. For the limited examples considered, it is observed that the rate at which the flutter boundary is approached is faster for the two composite panels than for the two isotropic panels.

The assumption often made that the eigenvectors encountered in structural dynamics are generally orthogonal may not always be the case when dealing with aeroelasticity in general, or the structural dynamics of aerospace vehicles in particular. It has been demonstrated in this study that the eigenvectors of systems encountered in aeroelasticity are not necessarily always orthogonal, and the angle between the nonorthogonal eigenvectors can be used to predict the onset of flutter. Thus, in the flutter control process and design, in which the response time is critical, the method based on eigenvectors seems to have its value if a means of early tracking of the eigenvectors is available. It appears desirable to explore further the potential application of this method to other engineering problems in which eigenvectors lose their orthogonality in the course of system dynamics.

References

[1] Crandall, S. H., and Mroszczyk, J. W., "Conservative and Nonconservative Coupling in Dynamic Systems," *Proceedings of the International Conference on Vibrations in Rotating Machinery*, Inst. of Mechanical Engineers, London, 1988, pp. 567–572.

[2] Afolabi, D., and Mehmed, O., "On Curve Veering and Flutter of Rotating Blades," *Journal of Engineering for Gas Turbines and Power*, Vol. 116, July 1994, pp. 702–708.

[3] Dowell, E. H., *Aeroelasticity of Plates and Shells*, Noordhoff International, Leyden, The Netherlands, 1975, Chap. 2.

[4] Arnol'd, V. I., "On Matrices Depending on Parameters," *Russian Mathematical Surveys*, Vol. 26, 1971, pp. 29–43.

[5] Afolabi, D., "Flutter Analysis Using Transversality Theory," *Acta Mechanica*, Vol. 103, Nos. 1–4, 1994, pp. 1–15.

[6] Bisplinghoff, R. L., and Ashley, H., *Principles of Aeroelasticity*, Dover, New York, 1962, Chap. 6.

[7] Fung, Y. C., "Some Recent Contributions to Panel Flutter Research," *AIAA Journal*, Vol. 1, No. 4, 1963, pp. 898–909.

[8] Dowell, E. H., "Panel Flutter: A Review of Aeroelastic Stability of Plates and Shells," *AIAA Journal*, Vol. 8, No. 3, 1970, pp. 385–399.

[9] Yang, H. T., Liaw, D. G., and Saigal, S., "Advances of Thin Shell Finite Elements and Some Applications," *Computers and Structures*, Vol. 35, No. 4, 1990, pp. 481–504.

[10] Pidaparti, R. M. V., and Afolabi, D., "The Role of Eigenvectors in Aeroelastic Analysis," *Journal of Sound and Vibration*, Vol. 193, No. 4, 1996, pp. 934–940.

[11] Pidaparti, R. M. V., and Yang, H. T., "Supersonic Flutter Analysis of Composite Plates and Shells," *AIAA Journal*, Vol. 31, No. 6, 1993, pp. 1109–1117.

[12] Yang, H. T., "Higher-Order Rectangular Shallow Shell Finite Elements," *ASCE, Journal of the Engineering Mechanics Division*, Vol. 99, No. 1, 1973, pp. 157–181.

[13] Guruswamy, P., and Yang, T. Y., "Aeroelastic Time Response Analysis of Thin Airfoils by Transonic Code LTRAN2," *Computers and Fluids Journal*, Vol. 9, No. 4, 1981, pp. 409–425.

A. Berman
Associate Editor